Erratum: Gate control, *g* factors, and spin-orbit energy of *p*-type GaSb nanowire quantum dot devices [Phys. Rev. B 103, L241411 (2021)]

Sven Dorsch, In-Pyo Yeo, Sebastian Lehmann, Kimberly Dick, Claes Thelander, and Adam Burke

(Received 21 February 2022; published 4 March 2022)

DOI: 10.1103/PhysRevB.105.119901

In our Letter, we use the wrongful assumption that in the bottom-gated quantum dot (QD) device the capacitive coupling between the gate electrode and the QD is sufficiently strong to pin the QD states energetically upon variation of an applied bias voltage V_{SD}. This assumption does not hold as can be seen by the slopes of the Coulomb diamond outlines in Fig. 3(a) of the main text. If the assumption was true, lines that exhibit a negative slope would be vertical and the observed finite slopes indicate a significant capacitive effect of a bias applied to the source contact on the QD states. As a consequence, a bias voltage induced QD level shift needs to be taken into account to translate the bias voltage along cutlines [labeled by dashed red lines in Fig. 3(b) of the main text] to an energy scale. Therefore, the energy axis in Fig. 3(c), Figs. 4(c) and 4(d), and Fig. S3 of the main text and the Supplemental Material are wrongfully scaled. In addition, the g^* factors presented in Fig. 3(d) as well as the extracted spin-orbit energies require rescaling. Aside from the erroneous data scaling addressed in this Erratum, the conclusions of our Letter hold and the g^* factors as well as the spin-orbit energy of our GaSb QD remain in a comparable range to other *p*-type nanowire systems but now fall short compared to those observed in InAs.

To account for the bias voltage induced level shift we geometrically extract the relevant bias voltage-to-energy conversion factor for each individual charge transition in Fig. 3(a). The conversion factor is given by the ratio of the real state splitting in units of energy, read out at the diamond edges, divided by the (zero B field) distance between QD states along vertical cutlines in units of the bias voltage. With the obtained conversion factors, we repeat the fits for the g^* factors as well as the spin-orbit energy and find for the fit in Fig. 3(c) of the main text $|g^*| = 0.7 \pm 0.1$. We further correct the spacings between the ground- and first excited orbital extracted from Figs. 4(a) and 4(b) in the main text to $\Delta\epsilon_{0,1} = 0.4$ and the spin-orbit energies to $\Delta_{SO} = 70 \pm 10\ \mu$eV and $\Delta_{SO} = 90 \pm 10\ \mu$eV, respectively. The updated fits given in Figs. 4(c) and 4(d) of the main text now yield $|g_0^*| = 1.0 \pm 0.2$, $|g_1^*| = 2.6 \pm 0.2$ and $|g_0^*| = 1.4 \pm 0.2$, $|g_1^*| = 2.9 \pm 0.2$, respectively. The additional state E_5 in Fig. 4(d) is introduced with $\Delta\epsilon_{1,2} = 0.16$ meV and $|g^*| = 1.6$.

In the following all erroneous panels of Figs. 3 and 4 of the main text as well as Fig. S3 of the Supplemental Material are shown with the correct scaling factors included. The revised g^* factors are shown in Fig. 3(d).

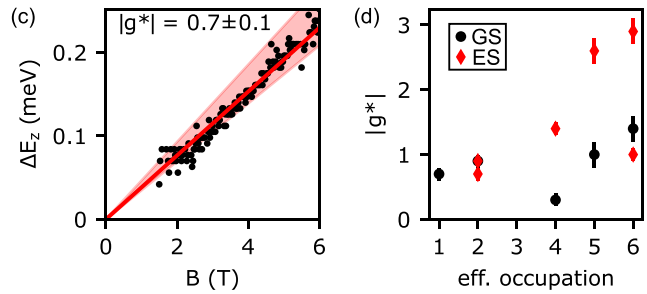

FIG. 3. (c) Fit to the Zeeman splitting ΔE_z extracted from (b). (d) $|g^*|$ for various ground-state (GS) and excited-state (ES) orbitals plotted against the effective occupation number of the QD, $p = 0$.

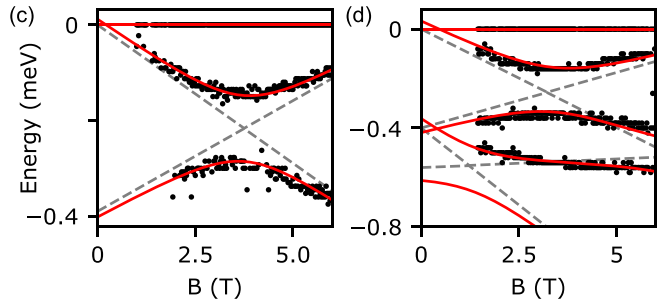

FIG. 4. (c), (d) Comparison and fit of data points extracted from (a) and (b), respectively, to calculated states with (solid red line) and without (gray dashed lines) level repulsion. All energies are normalized to the energetically highest ground state available for transport in the valence band.

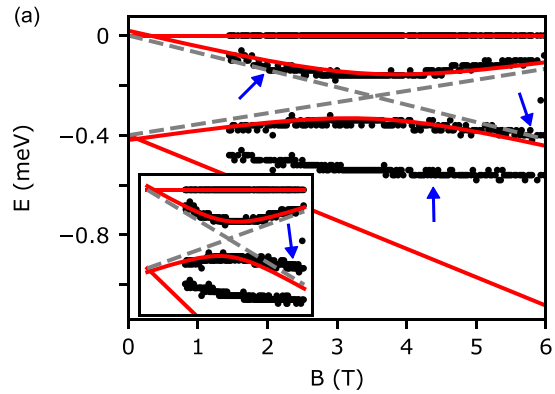

FIG. S3. (a) Fit to data points extracted from Fig. 4(b) in the main text with no additional state E_5. Only the lower branch of the ground- and upper branch of the first excited state is fitted, resulting in $|g_0^*| = 1.2$ and $|g_1^*| = 2.74$. Inset: Fit for only data of the lower ground state branch, resulting in $|g_0^*| = 1.39$ and $|g_1^*| = 3.06$. Blue arrows indicate discrepancies between the fit and the data.